Displacement Damage in Silicon due to Secondary Neutrons, Pions, Deuterons, and Alphas from Proton Interactions with Materials

Insoo Jun and William McAlpine(*)
Jet Propulsion Laboratory, California Institute of Technology, Pasadena CA 91109-8099
(*) Boeing Satellite Systems, El Segundo CA 90245

Abstract

The enhancement of displacement damage energy deposition due to secondary neutrons, pions, deuterons, and alphas resulting from high energy (100 - 1000MeV) proton interactions with aluminum and tungsten shielding are examined in this paper. The results obtained using a comprehensive Monte Carlo charged particle transport code, MCNPX Version 2.1.5, indicated that the dominant secondary particle is neutrons. The additional contribution to the displacement damage energy produced by secondary pions, deuterons, and alphas turned out to be less than 5%.

I. INTRODUCTION

Spacecraft systems in the natural space environment are subjected to various charged particles that include trapped electrons, trapped protons, galactic cosmic rays (GCR), and solar energetic particles (protons and other heavy ions). As particle energies become higher, their DeBroglie wavelength becomes short compared to the size of the target nucleus. Under these conditions, a new reaction type called spallation takes place in addition to the usual Coulomb and nuclear elastic/inelastic scattering. The products of the spallation reaction can be important for the accurate assessment of the radiation effects. The products include, but are not limited to, secondary protons, neutrons, pions, deuterons, and alphas. In this study, we investigated the effect of secondary particles (neutrons, pions, deuterons, and alphas) on

the displacement damage energy deposition in silicon resulted from high energy proton irradiation through aluminum and tungsten shields.

The displacement damage energy deposition can be computed if the particle spectrum and the Non-Ionizing Energy Loss (NIEL) of that particle as a function of energy are known. The NIEL plays the same role to the displacement damage energy deposition as the stopping power to the total ionizing dose (TID) [1]. Although there are some limitations in the usage of the NIEL concept [2], many studies have successfully shown that the degradation of semiconductor devices or optical sensors in a radiation environment can be linearly correlated to the displacement damage energy, and subsequently to the NIEL, deposited in the semiconductor devices or optical sensors [3-5].

The accurate calculation of displacement damage energy deposition in a material due to the high energy protons that include the contributions from secondary particles requires knowledge of the NIEL and the energy spectra of each relevant secondary particle species. There have been the studies where the effects of the secondary neutrons and/or secondary protons were extensively addressed [5,6]. However, the assessment for other species of secondary particles have not been easy, since their NIELs were not available, or there weren't any radiation transport codes that could compute the energy spectra of those secondary particles. Therefore, the effects of other secondary particles were often considered to be insignificant, or some arbitrary safety margins (30-50% on top of the neutron contribution) were applied to accommodate the uncertainty associated with neglecting their contribution to displacement damage energy deposition. This paper quantitatively addresses the displacement damage energy deposition from secondary pions, deuterons, and alphas for the first time, as well as from secondary neutrons. The displacement damage energy deposition calculations used published NIELs (references in Section III) and used the recently developed Monte Carlo charged particle transport code, MCNPX 2.1.5 [7].

II. PROBLEM SETUP

Only simple spherical shield geometry was considered in this study. The problem geometry consists of a 0.5-cm radius silicon sphere surrounded by various thicknesses of aluminum and tungsten. Aluminum and tungsten were chosen as the representative light (low/medium atomic number) and heavy (high atomic number) shielding materials that are commonly used in spacecraft construction (aluminum) and radiation shielding (tungsten). The shielding thicknesses ranged from 0.69 g/cm^2 to 20.6 g/cm^2 for both materials.

Spacecraft systems are typically exposed to energetic protons (particle energies > 10 MeV) as a result of solar particle events, or have mission profiles that cause the spacecraft to fly through or orbit planets with "belts" of magnetically trapped protons. The energy of the protons used in this study was limited to 100, 300, 500, and 1000 MeV. These proton energies are high enough to produce the secondary particles of interest, and are representative of the protons found in trapped in planetary magnetic fields or emitted during solar particle events. The 100, 300, 500 and 1000 MeV protons were assumed to be isotropically incident on the outer surface of the shielding material, and the volumetric displacement damage energy deposition over the silicon region was computed.

III. NON-IONIZING ENERGY LOSS (NIEL)

The displacement damage energy deposition can be computed if the Non-Ionizing Energy Loss (NIEL) and the particle spectrum are known in the region of interest. NIEL is a quantity that describes the rate of energy loss due to atomic displacement as a particle traverses a material, and can be calculated using the following analytical expression [6]:

$$S_{NIEL}(E) = \left(\frac{N}{A}\right)\sum_i \sigma_i(E)T_i \qquad (1)$$

where S_{NIEL} is the non-ionizing energy loss rate in MeV-cm^2/g, N is Avogadro's number, A is the gram atomic weight of the material, σ_i is the cross section of the i'th interaction, and T_i is effective average recoil energy corrected for ionization loss using the Lindhard theory [8]. Note that the unit of NIEL is the same as that of stopping power, and that the product of NIEL and the particle fluence gives the displacement damage energy per unit mass of material.

Figure 1 illustrates the NIELs used in this study for neutrons, protons, pions, deuterons, and alphas in the energy range of 1-1000 MeV. The NIELs for charged particles (protons, deuterons, and alphas) involve the consideration of atomic (Rutherford), nuclear elastic and nuclear inelastic reactions. There have been many studies for the proton-on-silicon NIELs (for example, see [6,9,10]). Among them, the NIELs in [6] is used in the present calculations. For the deuteron/alpha-on-silicon NIELs, the values reported in [11, and references therein] have been used.

As discussed in [12], the pion interaction is very different from other charged particle processes. For pion kinetic energies between 100 and 300 MeV, the interaction of pions with nucleons is dominated by the delta resonance production. The pion interaction with nuclei has another distinct feature that other charged particles do not have. Since the pion is a boson, it may not only undergo the usual scattering (Rutherford, nuclear elastic and nuclear inelastic), but may also disappear as a real pion within the nucleus by absorption. At higher energies, the particular features of the pion becomes less important, and the pion-nucleus interaction does not differ significantly from the scattering of any other charged particles by nuclei. All of these special features of the pion interaction had made the pion-on-silicon NIEL computation a little difficult, and thus only three evaluations [10,12,13] have been reported so far. Among them, Lazanu et. al. [12] computed the NIELs in the energy range of 50 MeV to 50 GeV by including all the pion reaction channels, and thus these values were used in this study. For the pion NIEL

between 1 and 50 MeV, the values reported by Huhtinen et. al. [13] were used. Huhtinen et. al., who adopted the proton data when estimating the inelastic contribution of pions to the NIEL, did not take explicitly into account the absorption, resulting in underestimation of the pion NIEL. However, as will be seen in the later section, the fact that the pion contribution to the total displacement damage energy deposition is not that significant validates the use of the Huntinen data.

The neutrons do not have charges so that they do not undergo Rutherford scattering. Only the nuclear elastic and inelastic scatterings are responsible for the NIEL. Recently, Jun [6] computed the neutron-on-silicon NIEL over the energy range of 1 to 1000 MeV by using the evaluated neutron microscopic cross sections (below 150 MeV) and kinematics (above 150 MeV), and those values are used in this paper.

IV. RESULTS AND DISCUSSION

Figures 2 to 5 summarize the results, respectively, for 100, 300, 500 and 1000 MeV proton irradiation into aluminum spherical shields, and Figures 6 to 9 illustrate the results for the tungsten cases. The number of the primary protons simulated for each case is between 3 to 12 millions to ensure that the uncertainties of the results are within 5%. A few observations are as follows: (1) Most of the secondary effects are due to neutrons, (2) The combined effects of secondary pions, deuterons, and alphas are small compared to the enhancement due to secondary neutrons, (3) The enhancement factor due to neutrons is much larger for tungsten than for aluminum for the same shield thickness in g/cm^2, (4) The secondary effects are more important for the higher energy protons than for the lower energy protons.

Therefore, the results showed that most of the secondary contributions are from the secondary neutrons, quantitatively justifying the reason why some of the previous studies concentrated solely on the secondary neutrons. The secondary pions, deuterons, and alpha particles produced from the high energy

proton interactions with aluminum or tungsten shielding account for a maximum of 5% enhancement in NIEL for very thick shielding applications.

V. CONCLUSIONS

The production of secondary protons and neutrons resulting from proton interactions with shielding media have been previously studied and used to determine end of life performance of critical electronics and sensors for both terrestrial and planetary spacecraft. Secondary pions, deuterons, and alpha particles produced by proton interactions have not been explicitly considered in spacecraft projects to date, but have been accommodated through adding additional margin, or possibly neglected. The maximum enhancement of 5% in displacement damage energy from secondary pions, deuterons, and alphas for extremely sensitive spacecraft electronics and sensors can now be used as a conservative bound rather than an arbitrary additional safety factor.

ACKNOWLEDGEMENT

The research described in this paper was carried out at the Jet Propulsion Laboratory, California Institute of Technology, under a contract with the National Aeronautics and Space Administration.

REFERENCES

1. G.P Summers et. al., "Displacement Damage Analogs to Ionizing Radiation Effects," Radiation Measurements, Vol. 24, No. 1, 1995
2. C.J. Marshall and P.W. Marshall, "IV. Proton Effects and TestIssues for Satellite Designers, Part B: Displacement Damage," in 1999 IEEE Nuclear and Space Radiation Effects Conference Short Course, Norfolk, Virginia, July 1999
3. G.R. Hopkinson et. al., "Proton Effects in Charged-Coupled Devices,", IEEE TNS, Vol. 43, No. 2, April 1996

4. J. Janesick et. al., "Radiation Damage in Scientific Charge-Coupled Devices," IEEE TNS Vol. 36, No. 1, February 1989

5. C. Dale et. al., "Displacement Damage Effects in Mixed Particle Environments for Shielded Spacecraft CCDs," IEEE TNS, Vol. 40, No. 6, December 1993

6. Insoo Jun, "Effects of Secondary Particles on the Total Dose and the Displacement Damage in Space Proton Environment," IEEE TNS, Vol. 48, No. 1, February 2001

7. L.S. Waters, Editor, "MCNPX™ User's Manual: Version 2.1.5", TPO-E83-G-UG-X-00001, Revision 0, Los Alamos National Laboratory, November 1999

8. J. Lindhard, V. Nielsen, M. Scharff, and P.V. Thomsen, "Integral Equations Governing Radiation Effects (Notes on Atomic Collisions, III)", Mat. Fys. Medd. Dan. Vid. Selsk., 33, N10, 1-42, 1963

9. E.A. Burke, "Energy Dependence of Proton-Induced Displacement Damage in Silicon", IEEE Transactions on Nuclear Science, Vol. NS-33, No. 6, pp. 1276-1281, December 1986

10. A. Van Ginneken, "Non Ionizing Energy Deposition in Silicon for Radiation Damage Studies," FN-522, Fermi National Accelerator Laboratory, October 1989

11. C. Dale and P. Marshall, "Displacement Damage in SI Imager for Space Applications," SPIE Vol. 1447 Charge-Coupled Devices and Solid State Optical Sensors II, pp. 70-86, 1991

12. I. Lazanu, S. Lazanu, U. Biggeri, E. Borchi, M. Bruzzi, "Non-Ionizing Energy Loss of Pions in Thin Silicon Samples," Nuclear Instruments and Methods in Physics Research A, Vol. 388, pp370-374, 1997

13. A. Huhtinen and P.A. Aarnio, " Pion Induced Displacement Damage in Silicon Devices," Nuclear Instruments and Methods in Physics Research A, Vol. 335, pp. 580-582, 1993

14. A. Van Ginneken, "Non Ionizing Energy Deposition in Silicon for Radiation Damage Studies," FN-522, Fermi National Accelerator Laboratory, October 1989

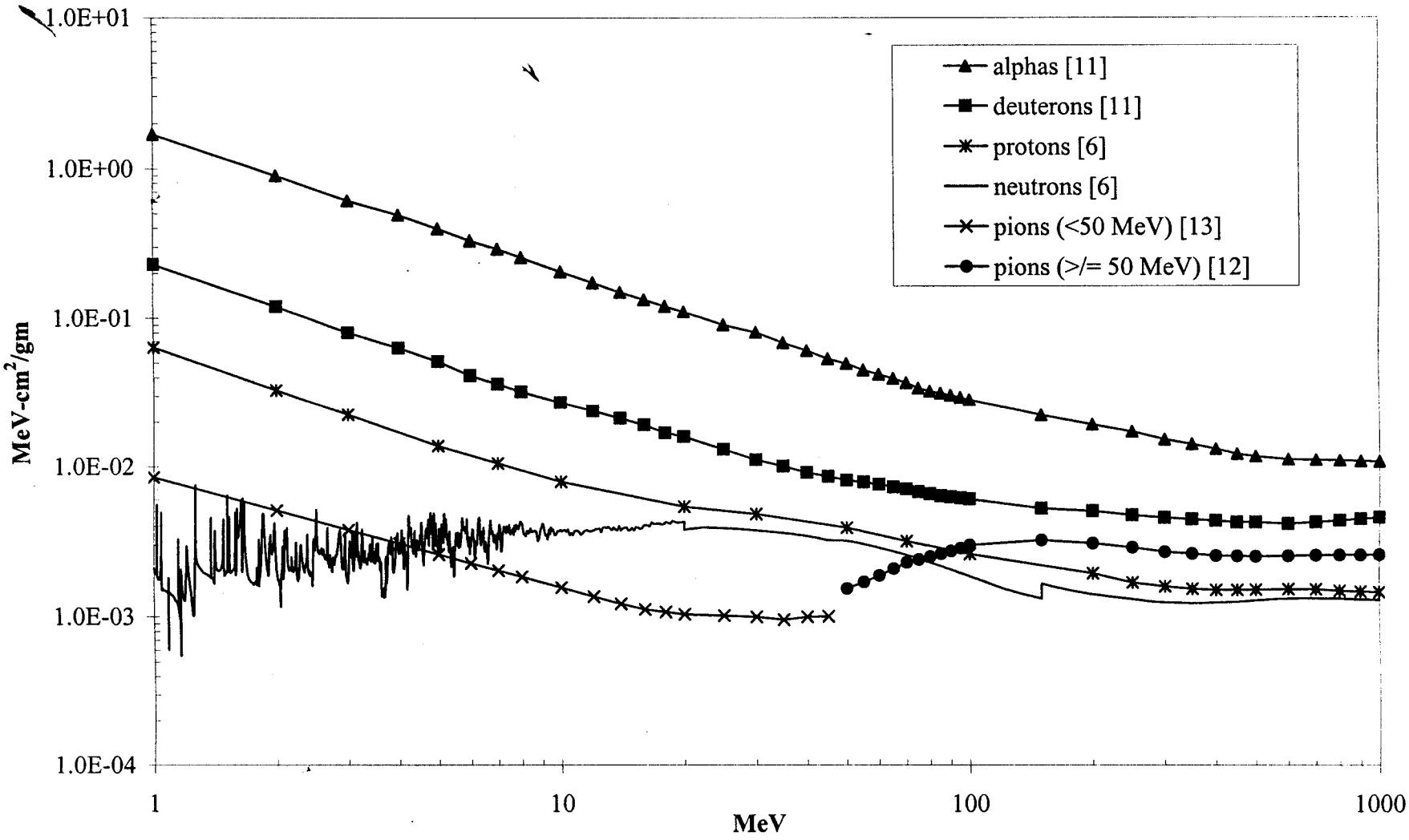

Figure 1. NIELs for various particles used in the present study

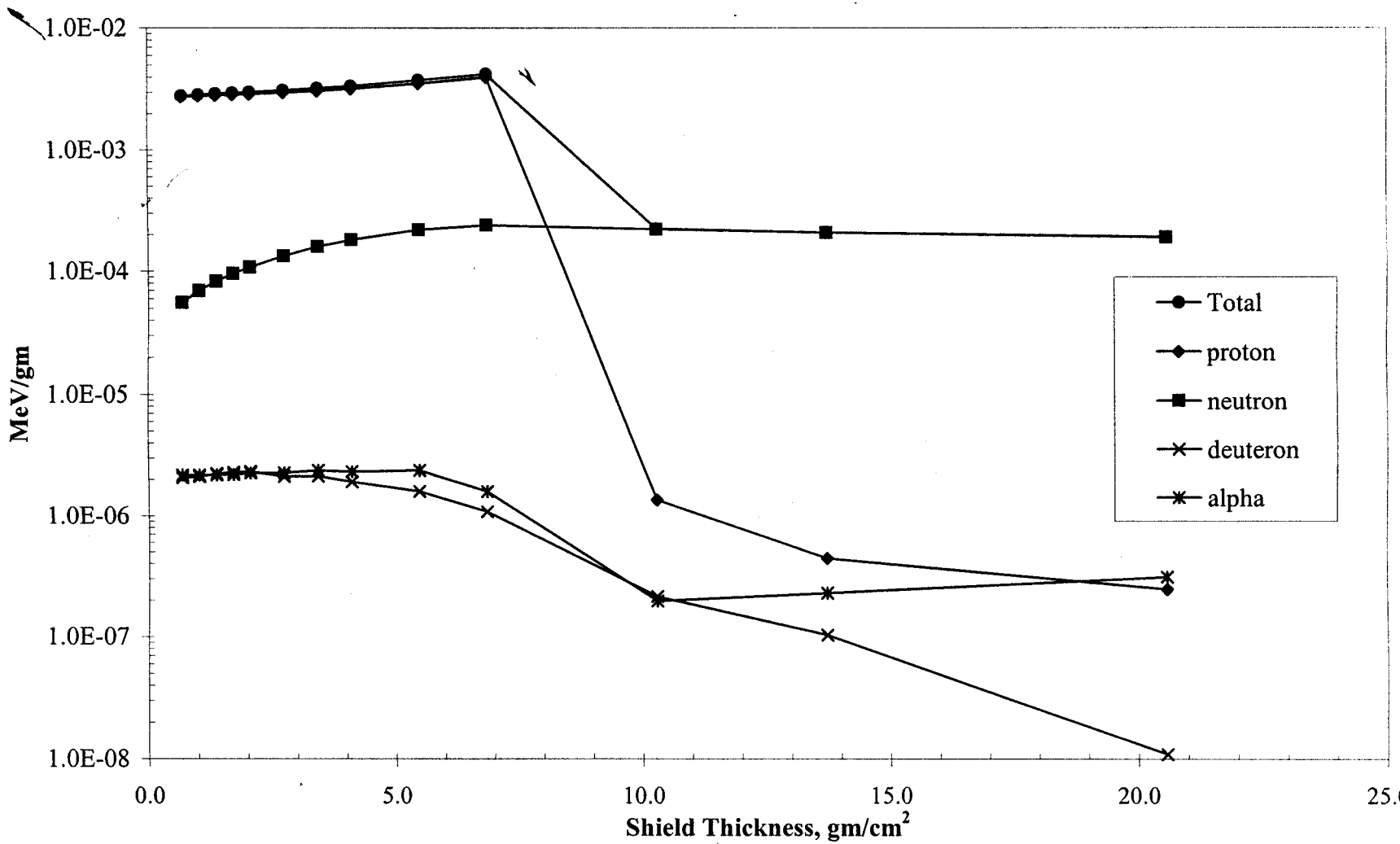

Figure 2. Displacement damage energy deposition profile normalized to 1 proton/cm^2 source strength as a function of aluminum shield thickness for isotropic 100 MeV protons. Error bars are not shown for clarity. The uncertainties of the results are less than 5%.

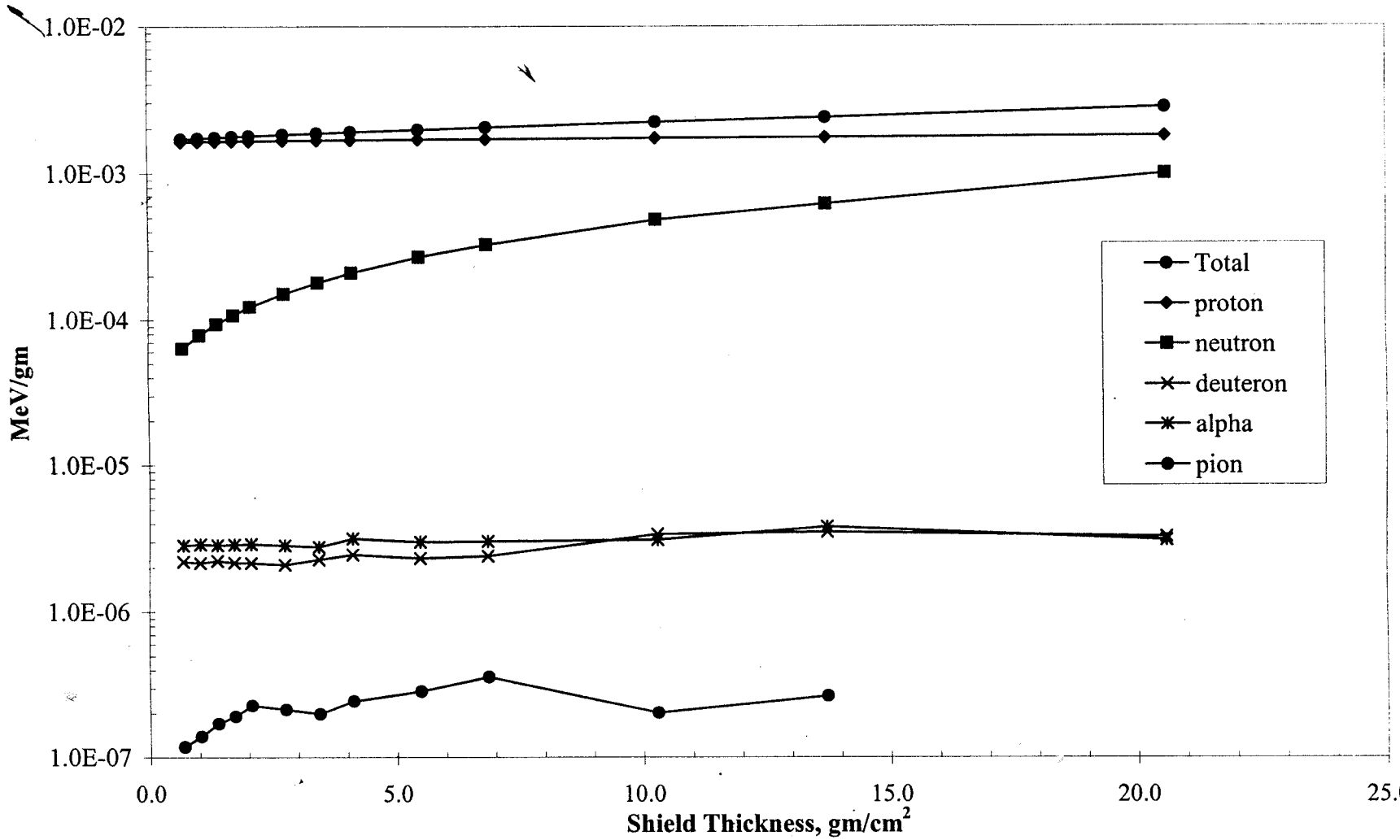

Figure 3. Displacement damage energy deposition profile normalized to 1 proton/cm^2 source strength as a function of aluminum shield thickness for isotropic 300 MeV protons. Error bars are not shown for clarity. The uncertainties of the results are less than 5%.

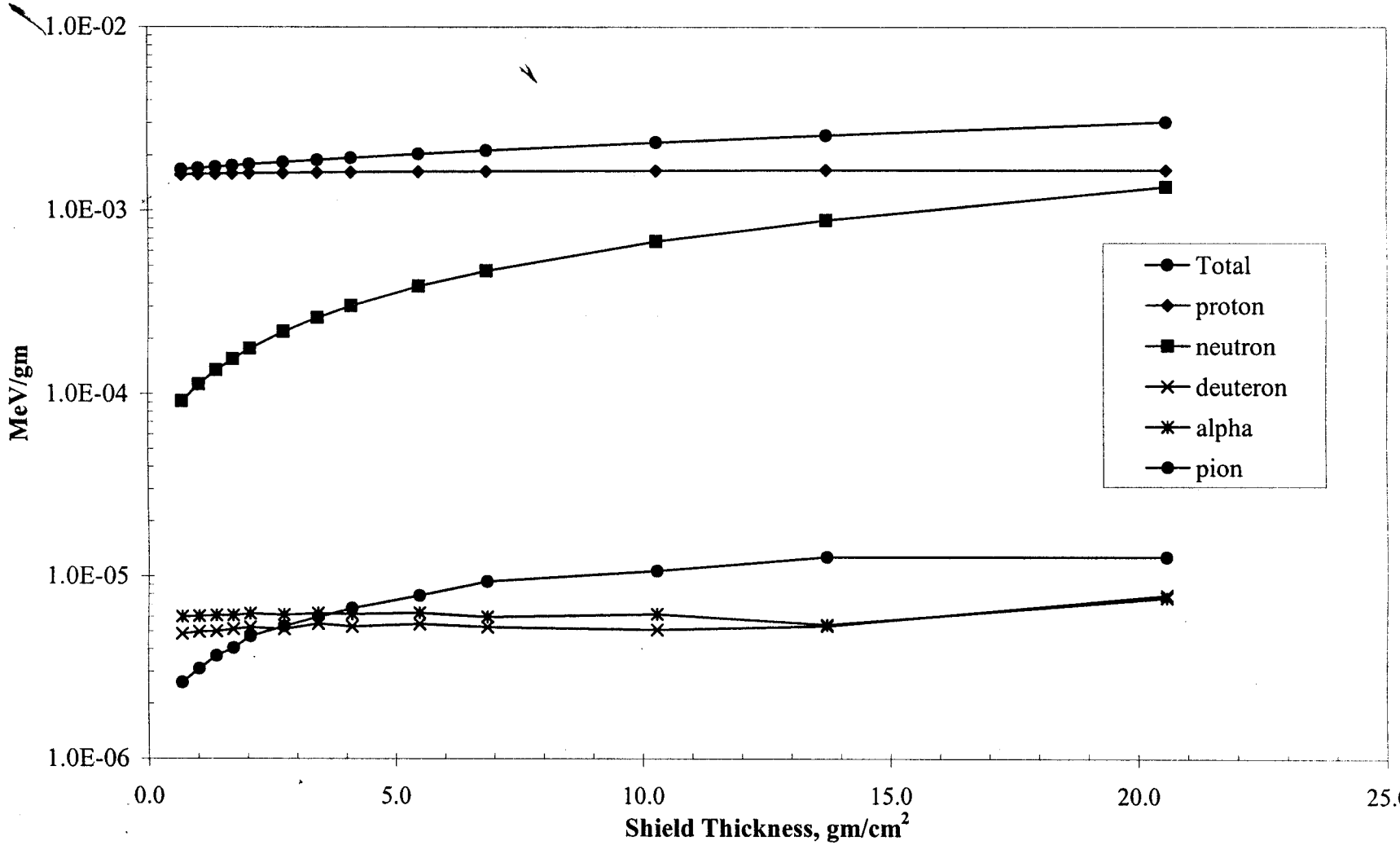

Figure 4. Displacement damage energy deposition profile normalized to 1 proton/cm^2 source strength as a function of aluminum shield thickness for isotropic 500 MeV protons. Error bars are not shown for clarity. The uncertainties of the results are less than 5%.

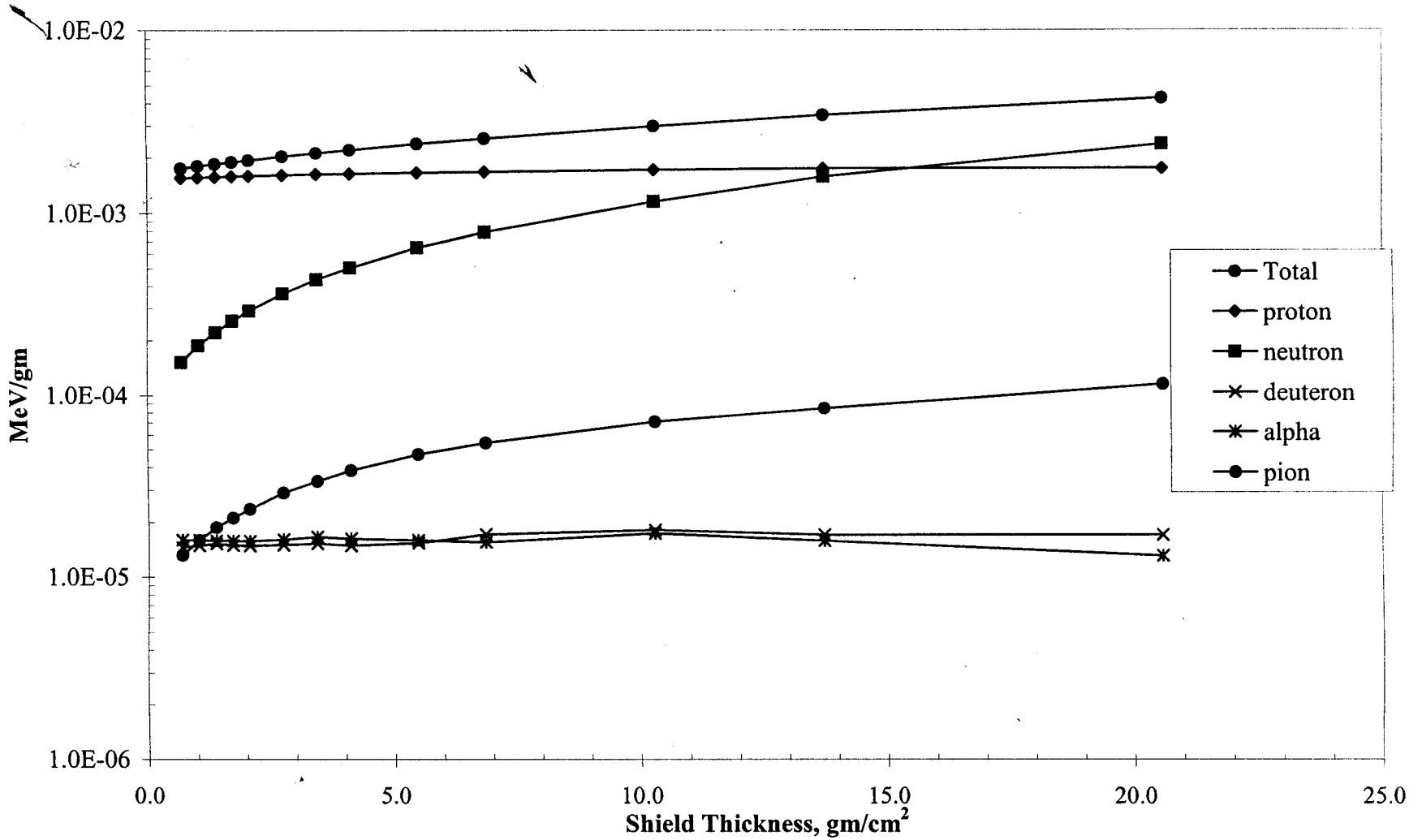

Figure 5. Displacement damage energy deposition profile normalized to 1 proton/cm^2 source strength as a function of aluminum shield thickness for isotropic 1000 MeV protons. Error bars are not shown for clarity. The uncertainties of the results are less than 5%.

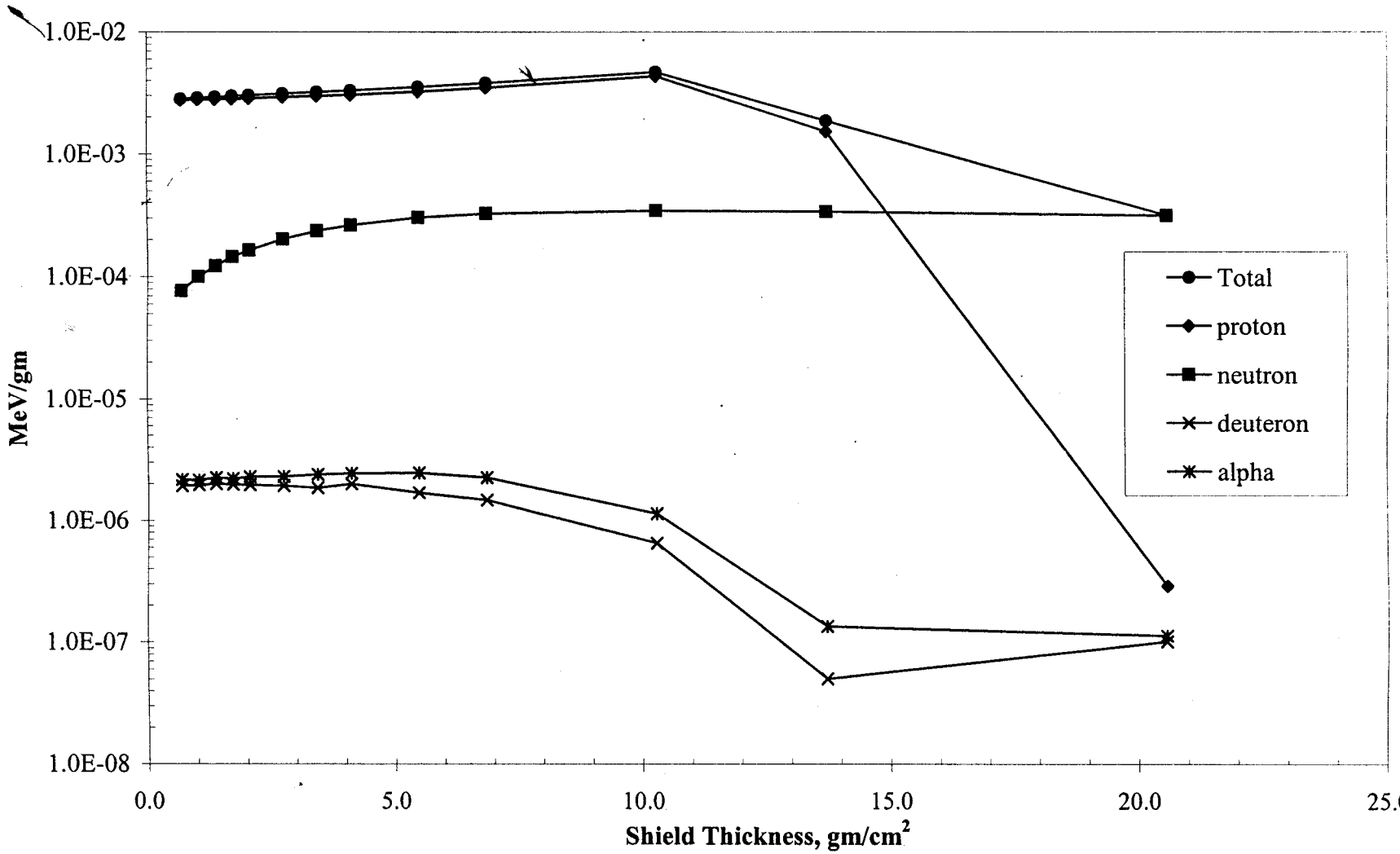

Figure 6. Displacement damage energy deposition profile normalized to 1 proton/cm^2 source strength as a function of tungsten shield thickness for isotropic 100 MeV protons. Error bars are not shown for clarity. The uncertainties of the results are less than 5%.

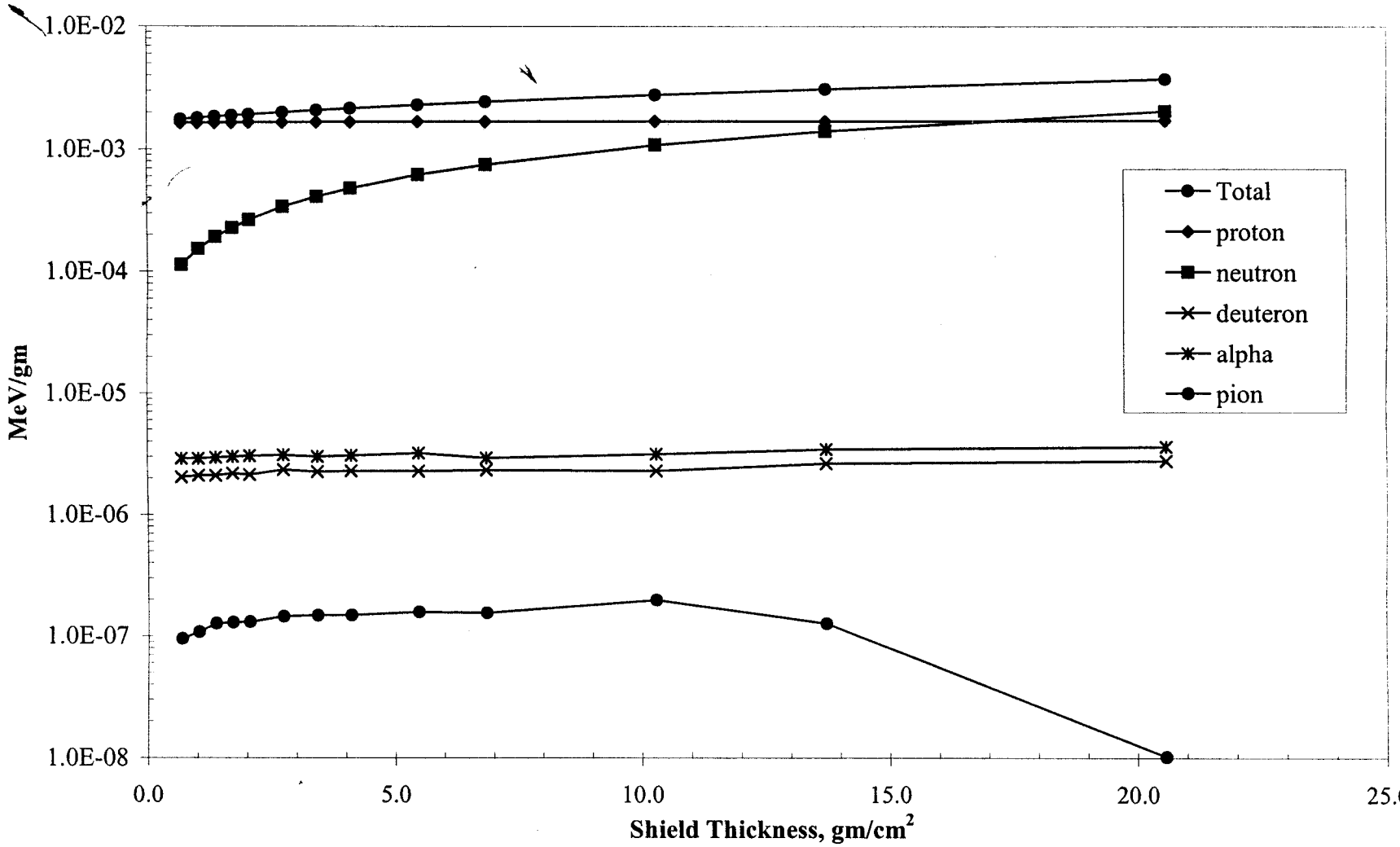

Figure 7. Displacement damage energy deposition profile normalized to 1 proton/cm^2 source strength as a function of tungsten shield thickness for isotropic 300 MeV protons. Error bars are not shown for clarity. The uncertainties of the results are less than 5%.

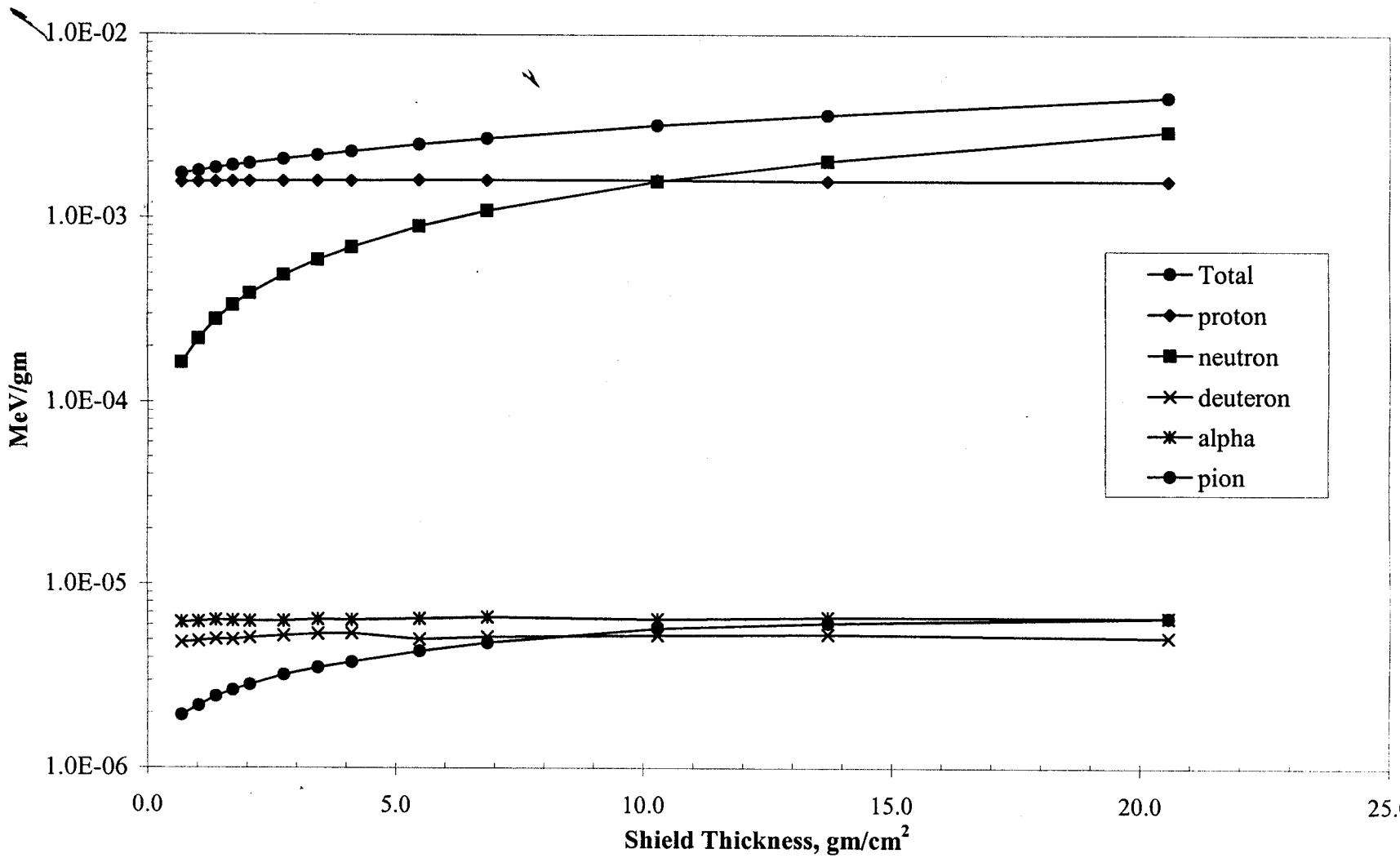

Figure 8. Displacement damage energy deposition profile normalized to 1 proton/cm^2 source strength as a function of tungsten shield thickness for isotropic 500 MeV protons. Error bars are not shown for clarity. The uncertainties of the results are less than 5%.

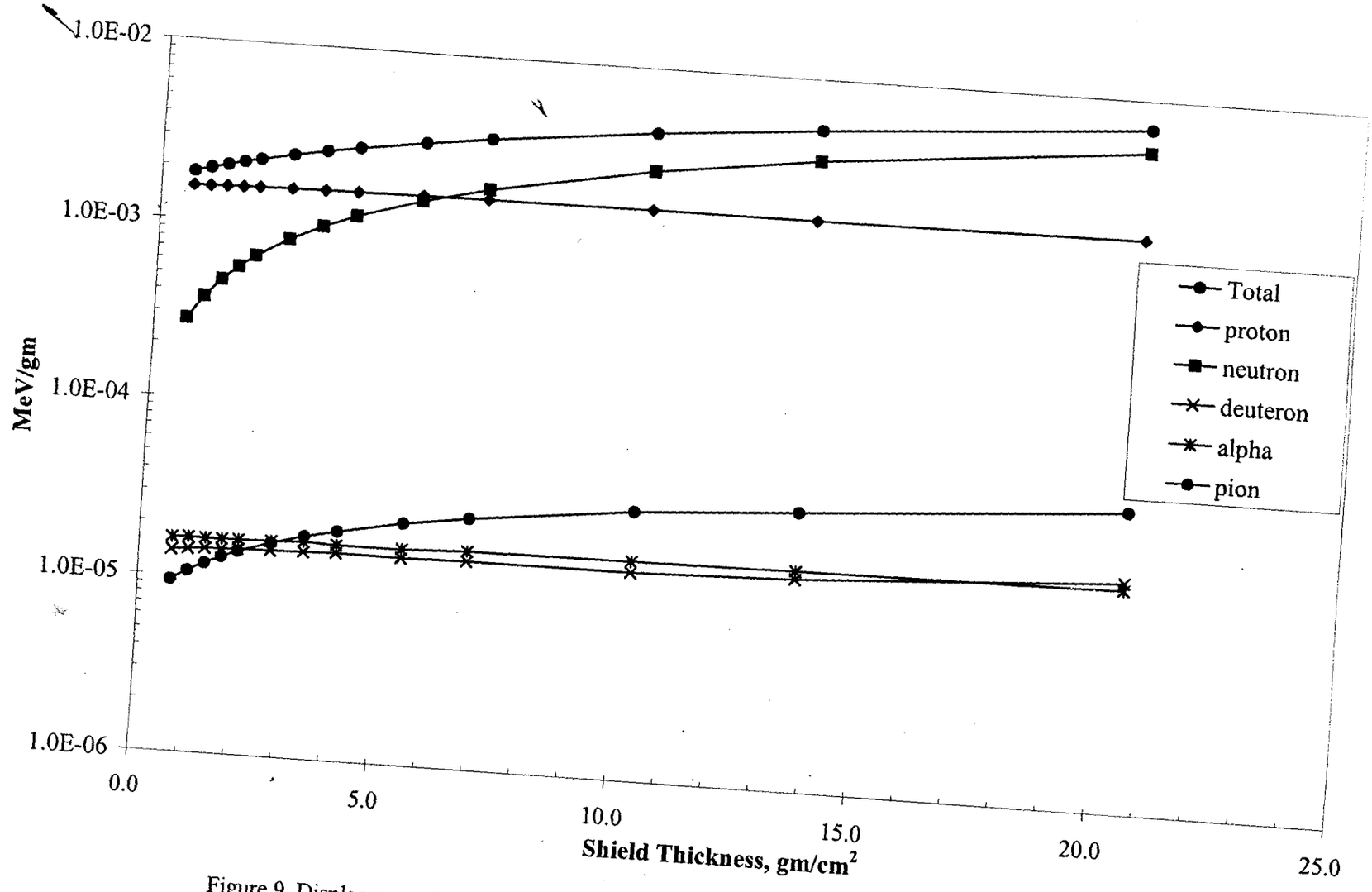

Figure 9. Displacement damage energy deposition profile normalized to 1 proton/cm^2 source strength as a function of tungsten shield thickness for isotropic 1000 MeV protons. Error bars are not shown for clarity. The uncertainties of the results are less than 5%.